Updated geology of the Clark Lakes area in central Yukon (parts of 106D/2, 3, 6 and 7)

Diane Skipton
Yukon Geological Survey

Liam Maw
Institut national de la recherche scientifique

Skipton, D. and Maw, L., 2021. Updated geology of the Clark Lakes area in central Yukon (parts of 106D/2, 3, 6 and 7). *In:* Yukon Exploration and Geology 2020, K.E. MacFarlane (ed.), Yukon Geological Survey, p. 73–94.

Abstract

The Clark Lakes area is located along the northern boundary of the Selwyn fold belt, and is underlain by the Ediacaran to Cambrian Hyland Group. In the surrounding region, the Hyland Group and Paleozoic platformal carbonate rocks host several Au and polymetallic mineral deposits. The Clark Lakes area is bordered by regional-scale, southeast-striking thrust faults, which include the Dawson thrust to the northeast, and the Tombstone and Robert Service thrusts to the southwest. Based on stratigraphic relationships identified during 1:50 000-scale bedrock mapping, Hyland Group rocks in the Clark Lakes area are considered to belong to the Cryogenian–Ediacaran Yusezyu Formation, the Ediacaran Algae Formation and the Ediacaran–Terreneuvian Narchilla Formation. The Yusezyu Formation has been subdivided into five units based on dominant siliciclastic lithofacies, which form a broadly coarsening-upward sequence. The Yusezyu and Narchilla formations host gabbro sills, and quartz monzonite occurs locally in the upper Yusezyu Formation. Rocks in the Clark Lakes area exhibit a steeply northeast-to-southwest-dipping foliation that is axial planar to southeast-trending folds.

* diane.skipton@yukon.ca

Introduction

This article presents the results of 1:50 000-scale bedrock mapping conducted in 2019 in the Clark Lakes area of central Yukon, which includes parts of NTS sheets 106D/2, 3, 6 and 7. The Clark Lakes area is located along the northern boundary of the Selwyn fold belt, where the Neoproterozoic–Cambrian Hyland Group is juxtaposed against Paleozoic slope and shelf rocks of the Ogilvie Platform along the Dawson thrust zone (Figs. 1 and 2; Green, 1972a,b; Colpron et *al.*, 2013). The surrounding region hosts several mineral deposits (Fig. 2), including carbonate-hosted intrusion-related Au-Ag (Tiger), epithermal Ag-Au-Pb-Zn (McKay Hill), manto Ag-Pb-Zn (Clark), plutonic-related Au-Ag (Dublin Gulch), vein polymetallic Ag-Pb-Zn (Keno) and volcanogenic massive sulphide Au-Cu-Zn-Pb (Marg).

The region was initially mapped at 1:250 000-scale by the Geological Survey of Canada (Green, 1972a,b) as part of a helicopter-supported mapping project that included the Nash Creek, Larsen Creek and Dawson areas (Green, 1972a,b). More detailed (1:50 000-scale) bedrock mapping was undertaken in the Clark Lakes area in 2019 as part of a multi-year mapping and research project to address outstanding questions regarding stratigraphy, structural history and mineral potential.

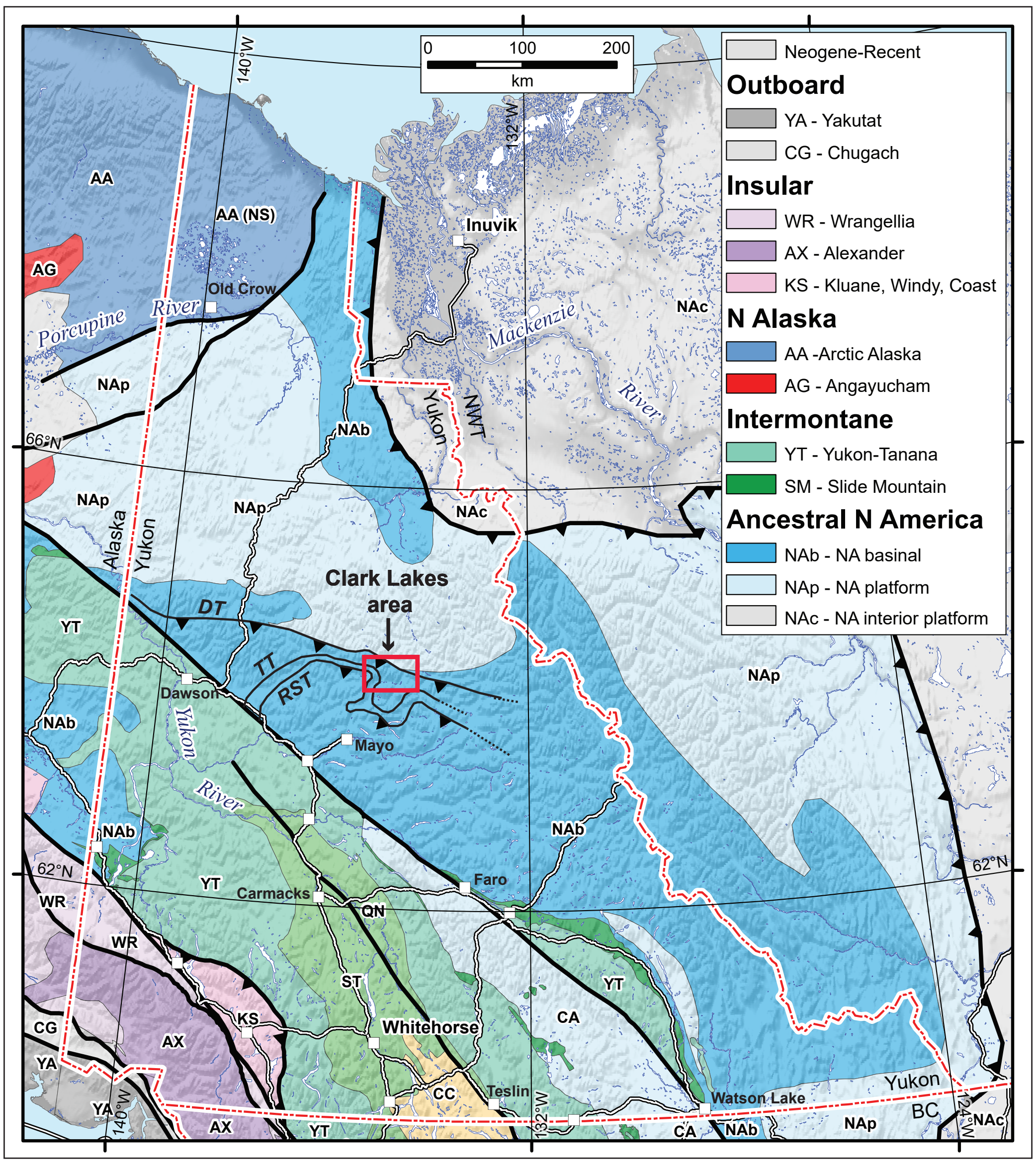

Figure 1. Map of the geological terranes that comprise the northern Cordillera (Colpron et al., 2007). The study area (Clark Lakes area) is located in central Yukon, and outlined in red. DT = Dawson thrust; TT = Tombstone thrust; RST = Robert Service thrust.

Geological setting and previous work

Previous mapping of the Clark Lakes area (Green, 1972a,b) showed that it is mostly composed of the Neoproterozoic Hyland Group (Fig. 2), including siliciclastic rocks of the Yusezyu Formation, with lesser carbonate rocks of the Algae Formation. On the geological compilation map of Yukon (Yukon Geological Survey, 2020a), the Hyland Group is juxtaposed over Carboniferous–Permian clastic rocks (Tsichu(?) Group) and Upper Cambrian–Devonian platformal carbonate rocks (Bouvette Formation) across the Dawson thrust zone (Fig. 2). The northeast-vergent Dawson thrust zone extends northwest–southeast across central Yukon, from the Ogilvie Mountains to the eastern Wernecke Mountains (Fig. 1). It records a protracted history that may have begun in the Neoproterozoic, with reactivation in the Paleozoic, and during Mesozoic (mid-Cretaceous?) shortening associated with Cordilleran orogenesis (Abbott, 1997c; Colpron *et al.*, 2013). Southwest of the Clark Lakes area, the Hyland Group is juxtaposed against the Devonian–Mississippian Earn Group along the Robert Service thrust, and the Earn

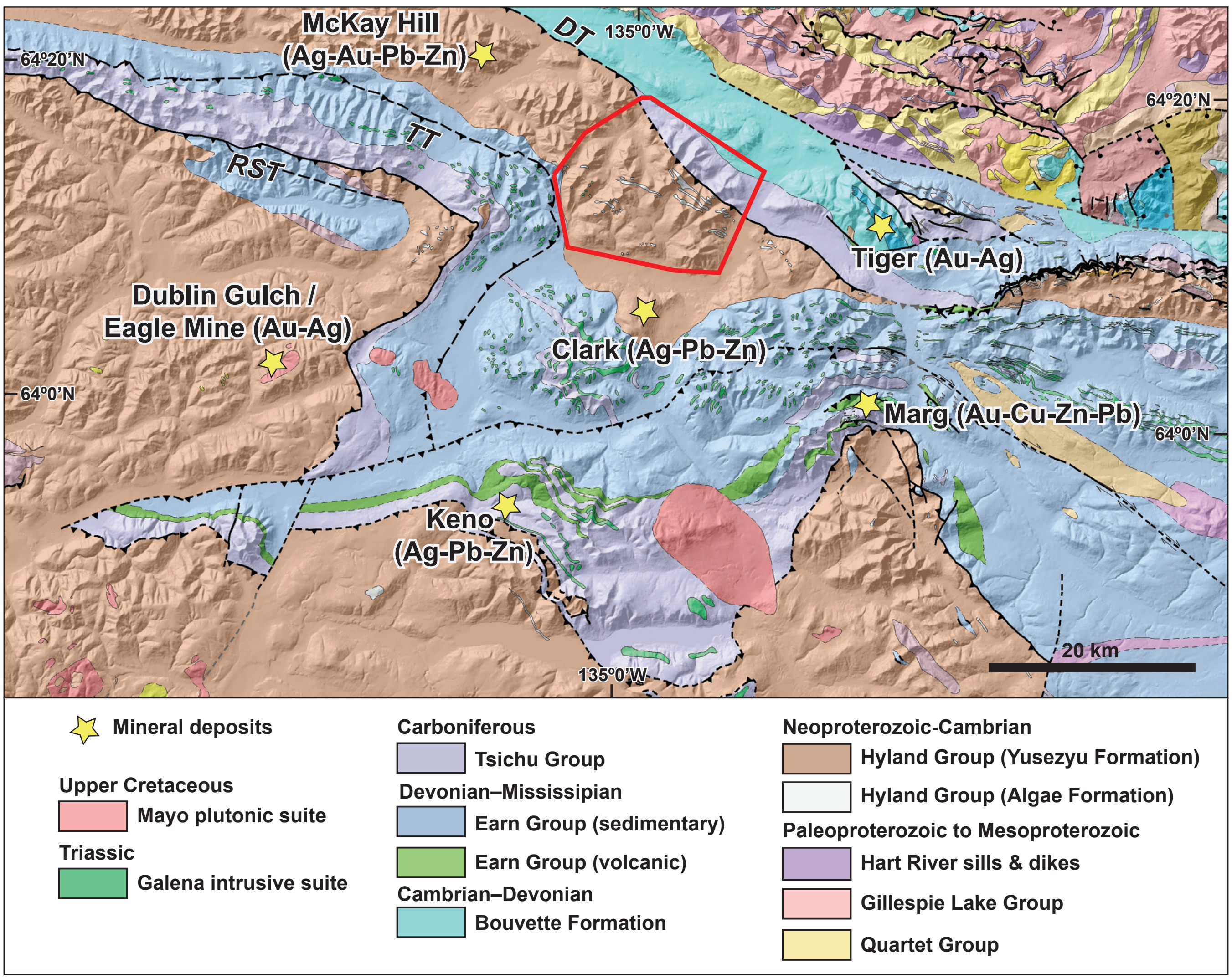

Figure 2. *Geological map of Paleoproterozoic to Carboniferous strata and younger plutons in the region of the Keno, Tiger and McKay Hill mineral deposits in central Yukon (from the digital compilation map of Yukon; Yukon Geological Survey, 2020a). The area mapped in 2019 (the Clark Lakes area; this study) is outlined in red, and was initially mapped at 1:250 000-scale (Green, 1972a). DT = Dawson thrust; TT = Tombstone thrust; RST = Robert Service thrust.*

Group is repeated by the Tombstone thrust (Figs. 1 and 2; Green and Roddick, 1962; Tempelman-Kluit, 1970; Thompson *et al.*, 1990; Anderson, 1987; Roots, 1988; Murphy, 1997). The southern and western edges of the Clark Lakes area are bordered by the Tombstone high-strain zone, a several-km thick interval of intensely deformed, lower-to-middle-greenschist-facies metasedimentary rocks (Devonian Earn Group, Mississippian Keno Hill Quartzite) in the hanging wall of the Tombstone thrust (Murphy, 1997). Shear-sense indicators in the Tombstone high-strain zone record top-to-the-northwest displacement (Murphy, 1997). Muscovite from the hanging wall of the Robert Service thrust, which is within the Tombstone high-strain zone, yielded $^{40}Ar/^{39}Ar$ dates of *ca.* 104–100 Ma, interpreted as the age of latest deformation (Mair *et al.*, 2006). The Clark Lakes area is considered to have reached lower-greenschist-facies (chlorite zone) conditions, in contrast with the sub-greenschist-facies conditions of the Hyland Group in the eastern Wernecke Mountains (Read *et al.*, 1991).

Several 1:50 000 and 1:75 000-scale mapping projects have improved our understanding of regional stratigraphic and structural relationships across the Dawson thrust zone in the Ogilvie and Wernecke mountains (Abbott, 1990a,b, 1997a,b,c; Colpron *et al.*, 2013; Moynihan, 2014, 2016a) and across the Tombstone and Robert Service thrust zones in the McQuesten River and Mayo areas (Murphy, 1997; Roots, 1997). However, due to less detailed (1:250 000-scale) mapping in the Clark Lakes area, the structural architecture of the area and stratigraphic correlations with Selwyn basin rocks elsewhere remained uncertain. Determining the structural and thermal history of the Clark Lakes area, and potential links with the major bounding thrust systems, is important for reconstructing the regional tectonic history and the geological setting of mineral deposits in the Dawson and Tombstone–Robert Service fault corridors. The 1:50 000-scale bedrock mapping of the Clark Lakes area is supported by new aeromagnetic data in the region (Kiss, 2020).

Stratigraphy

The Clark Lakes area mainly consists of siliciclastic and carbonate strata that have been tilted towards the southwest, such that the oldest rocks are closest to the Dawson thrust (Fig. 3). Based on lithofacies mapping and comparisons with stratigraphic relationships in the broader Selwyn basin (*e.g.*, the eastern Wernecke Mountains and the Hyland River area; Colpron *et al.*, 2013; Moynihan, 2014, 2016b), the strata are considered equivalent to the Cryogenian–Ediacaran Yusezyu Formation, the Ediacaran Algae Formation and the Ediacaran–Terreneuvian Narchilla Formation of the Hyland Group. This interpretation is supported by U-Pb detrital zircon dating of sandstone in the Clark Lakes area, which yielded maximum depositional ages of *ca.* 665–725 Ma and detrital zircon populations that are similar to those of the Yusezyu Formation elsewhere in the Selwyn basin (J. Crowley and D. Skipton, unpublished data, 2020). Nonetheless, stratigraphic correlations between the Clark Lakes rocks and the Yusezyu, Algae and Narchilla formations are considered to be preliminary, and may be refined following additional bedrock mapping.

Hyland Group: Yusezyu Formation

The Clark Lakes area is dominantly underlain by siltstone, shale and sandstone of the Yusezyu Formation. The Yusezyu Formation exhibits an overall coarsening-upwards succession across the map area, whereby shale and siltstone-dominated sequences in the northeast grade upwards into more sandstone-rich units towards the southwest (Fig. 3). The Yusezyu Formation has been subdivided into five units based on predominant lithofacies. At the stratigraphically lowest level along the northeastern edge of the map area, the Yusezyu Formation is shale-dominated (PHYsh) and consists of grey, dark grey and green shale (mudstone) that is homogeneous to thinly laminated and locally phyllitic (Fig. 4a,b). In places, the shale contains thin, rhythmic interbeds of grey siltstone. The shale-dominated unit exhibits a gradational upper contact with a slightly coarser-grained, siltstone-dominated unit (PHYsl) of the Yusezyu Formation; observed thicknesses of these units are estimated to be approximately 2 km and 1.5 km, respectively. The siltstone-dominated unit is mostly composed of green to grey siltstone to phyllite, which locally contain dark green-grey mudstone laminations or interbeds (Fig. 4c). The siltstone-dominated unit includes minor amounts of thin to medium-bedded, white siltstone to fine-grained sandstone, as well as dark grey and green shale (Fig. 4d). The contact between the Yusezyu Formation siltstone-dominated unit (PHYsl) and the overlying Yusezyu Formation "mixed" unit (PHYm) is marked by the first (*i.e.*, stratigraphically deepest) occurrence of medium-grained quartz arenite or quartz grit sandstone. The Yusezyu Formation mixed unit is the most predominant unit in the Clark Lakes area (Fig. 3), and is estimated to have an observed (deformed) thickness of approximately 800–1200 m. It consists of a heterogeneous mixture of siltstone (~55%), shale (~30%), and sandstone (~15%; Fig. 5a). These lithologic units typically form alternating intervals that are ~3 m to 10s of metres thick. Locally, sandstone and siltstone are rhythmically interbedded, forming medium to thick beds. The Yusezyu Formation mixed unit includes green and grey siltstone to phyllite; dark grey, green and, locally, maroon shale; and minor amounts of brown to grey quartz arenite and quartz grit, with local quartz-pebble conglomerate. The mixed unit also contains thick (up to ~500 m) intervals of sandstone (PHYss and PHYsc) that are laterally discontinuous and are interpreted to represent discrete channel deposits. Sandstone locally exhibits ripple cross-laminations or cross-bedding. The most abundant Yusezyu Formation sandstone unit (PHYss) is composed of medium to thick-bedded, brown to grey quartz arenite and quartz grit with local quartz-pebble conglomerate (Fig. 5b–e), and rare dark grey and green shale and siltstone to phyllite. The subordinate Yusezyu Formation sandstone unit (PHYsc) is distinguished by local dolomitic cement in sandstone, higher proportions of shale, siltstone and phyllite, and by rare intervals (<3 m thick) of limestone and dolostone.

Hyland Group: Algae Formation

The upper Yusezyu Formation (PHYm, PHYss, PHYsc) is overlain by the Algae Formation (PHa) along a sharp contact. The Algae Formation contains predominantly grey, fine-grained, massive to medium-bedded limestone (Fig. 6a,b) with local laminations, and lesser amounts of fine-grained, orange-weathered, medium-bedded dolostone. The Algae Formation in the Clark Lakes area has an estimated observed thickness of approximately 30–50 m, although the thickness is uncertain in places due to complex fold geometries (Fig. 3). As it is readily distinguishable from the Hyland Group siliciclastic rocks, the Algae Formation was used as a marker horizon for mapping. Additionally, the distinctive light grey weathering colour of the Algae Formation facilitated remote mapping of inaccessible areas, where exposure allowed, and enabled identification of complex, map-scale folds (Figs. 3b and 10e) that may otherwise have been masked within interbedded siliciclastic strata.

Hyland Group: Narchilla Formation

The Narchilla Formation (PCHn) overlies the Algae Formation along a sharp contact. The Narchilla Formation mostly consists of fine-grained siliciclastic rocks, including dark grey, green and maroon shale (Fig. 6c), and grey to green siltstone to phyllite (Fig. 10a). It contains lesser amounts of fine-grained, white, thinly bedded sandstone with local ripple cross-laminations (Fig. 6d), interbedded green-grey to white, fine-grained sandstone and siltstone (Fig. 10b), and rare occurrences of brown to grey quartz arenite and quartz grit. In the eastern Wernecke Mountains and the Hyland River area, the Narchilla Formation is sharply overlain by limestone conglomerate (or limestone) of the Gull Lake Formation (Moynihan, 2014, 2016b). In the Clark Lakes area, the Narchilla Formation represents the highest stratigraphic level of exposure, and its exposure is mostly limited to synclinal keels (Figs. 3 and 10e). As such, the thickness of the Narchilla Formation is poorly constrained in the map area, but it is estimated to be at least 500 m thick.

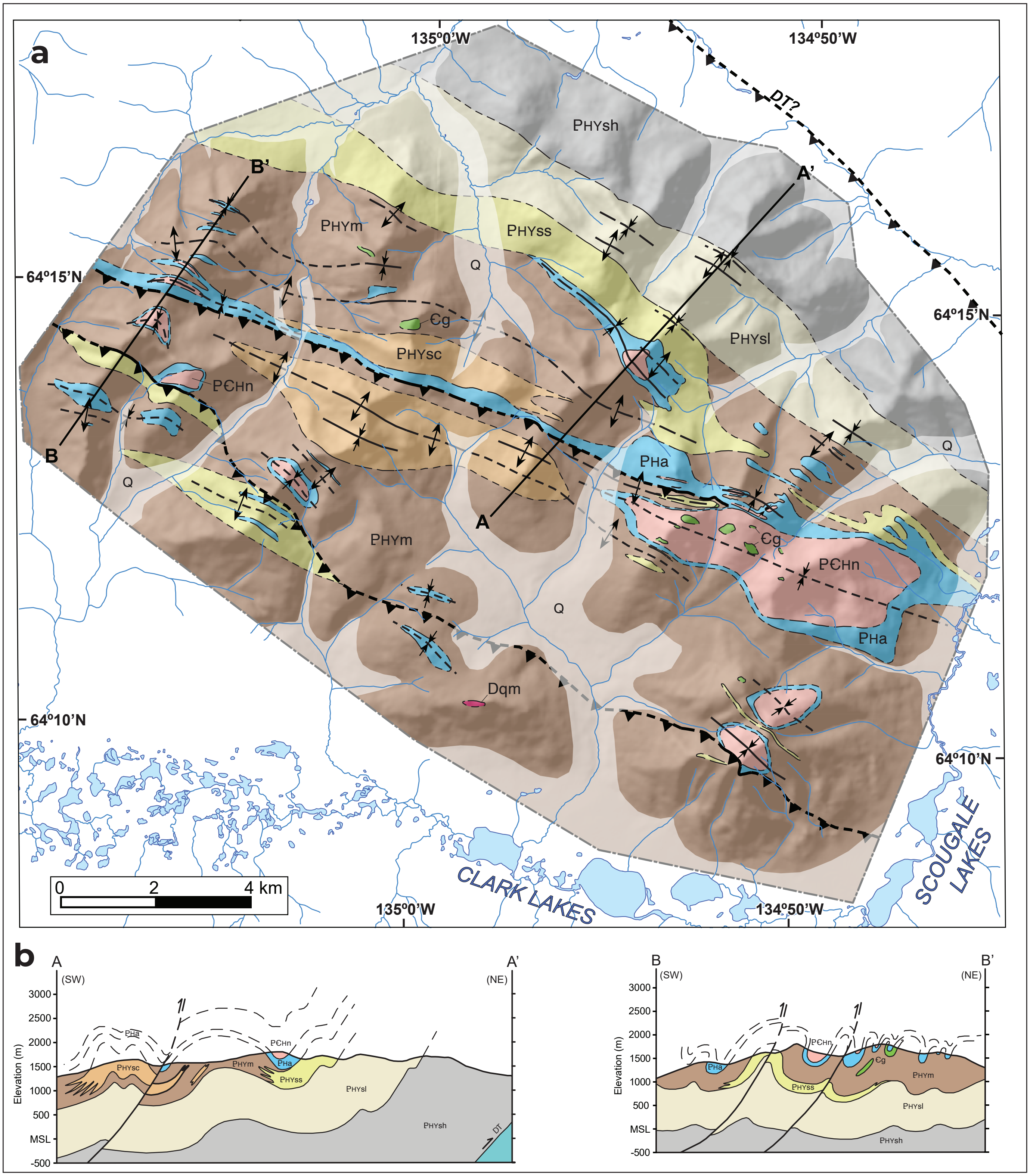

Figure 3. ***(a)*** *Preliminary geological map of the Clark Lakes area (parts of NTS 106D/2, 3, 6, 7) based on 1:50 000-scale bedrock mapping conducted in 2019. Map legend is provided in Figure 3c. DT?, inferred trace of Dawson thrust zone.* ***(b)*** *Cross sections corresponding to the preliminary geological map of the Clark Lakes area in Figure 3a. In cross section A-A', the location of the Dawson thrust zone (DT) is projected at depth from the estimated location of the thrust at surface (Fig. 3a).*

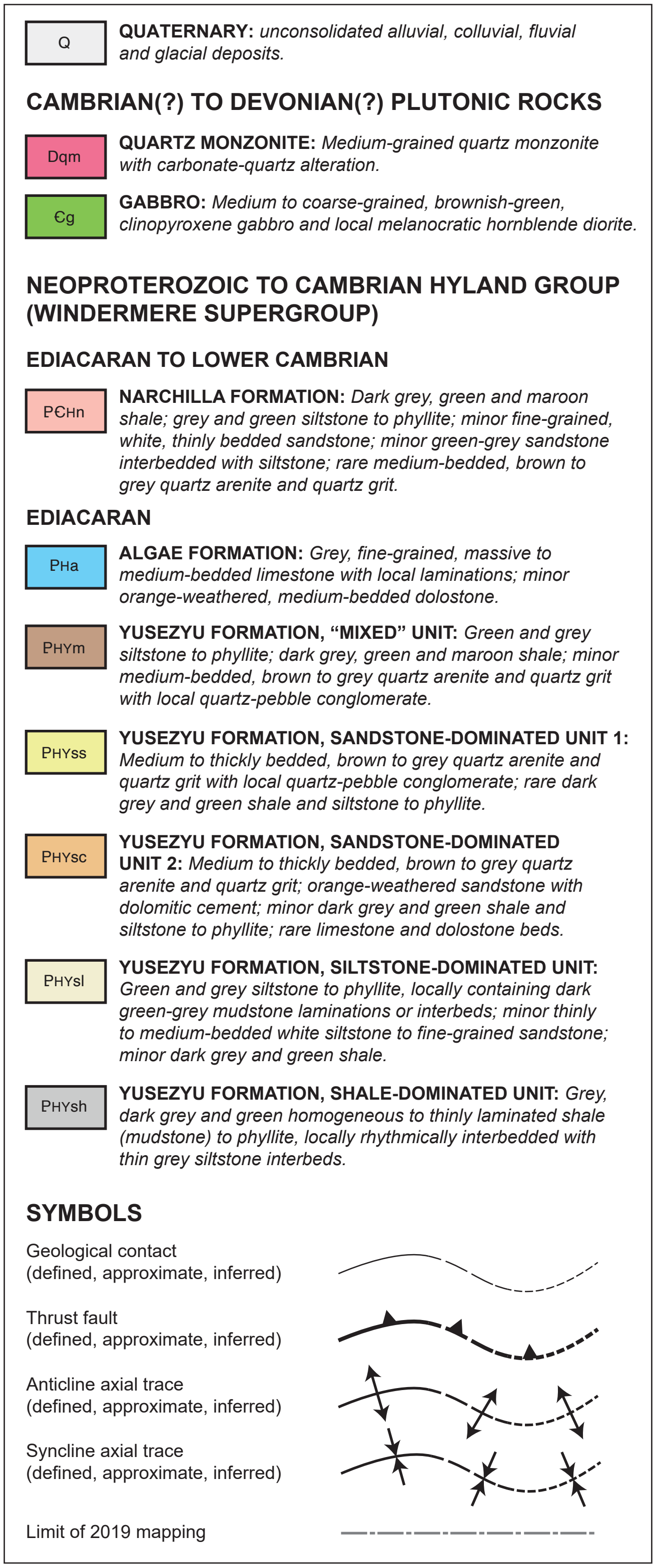

***Figure 3. (c)** Legend corresponding to the preliminary geological map of the Clark Lakes area in Figure 3a.*

Intrusive rocks

Gabbro

Gabbro intrusions (Єg) were emplaced into siltstone and shale of the Narchilla and upper Yusezyu formations on the eastern side and northwestern quadrant of the map area (Fig. 3). The intrusions form discontinuous sills and plugs with maximum dimensions estimated to be ~200 m at the bedrock surface (Fig. 7a). Gabbro is medium-grained, locally foliated, and has been extensively replaced by greenschist-facies minerals (chlorite, actinolite, epidote) and carbonate alteration (Fig. 7b,c). Igneous textures have been preserved locally, and relics of igneous clinopyroxene crystals are visible in thin section. In some places, igneous hornblende occurs instead of clinopyroxene, indicating that the intrusions have a compositional range from gabbro to, locally, melanocratic hornblende diorite. As the intrusions are hosted by the Narchilla Formation, they are inferred to be Terreneuvian or younger.

Whole rock geochemical compositions of the gabbro and hornblende diorite intrusions (Table 1) suggest that most (five) of the samples have alkali basaltic compositions that are transitional between those of typical oceanic island basalt and enriched mid-ocean ridge basalt (Fig. 8). Preliminary geochemical comparisons with Cambrian and younger mafic to intermediate rocks in the region (using data from: Abbott, 1997c; Yukon Geological Survey, 2020b; M. Colpron, pers. comm., 2020) suggest that the Clark Lakes gabbro and diorite are distinct from the Triassic Galena suite sills hosted by the nearby Earn Group. Instead, they may share affinity with Paleozoic sills, dikes and volcanic rocks (Dempster Volcanics), such as those in the Upper Hart River area (Abbott, 1997c; Yukon Geological Survey, 2020b). A sixth gabbro sample (19DS-115-2-1) from the Clark Lakes area is geochemically distinct, as it has a trachyte-phonolite composition and is enriched in several rare earth elements by an order of magnitude relative to the other gabbro and hornblende diorite samples (Table 1; Fig. 8).

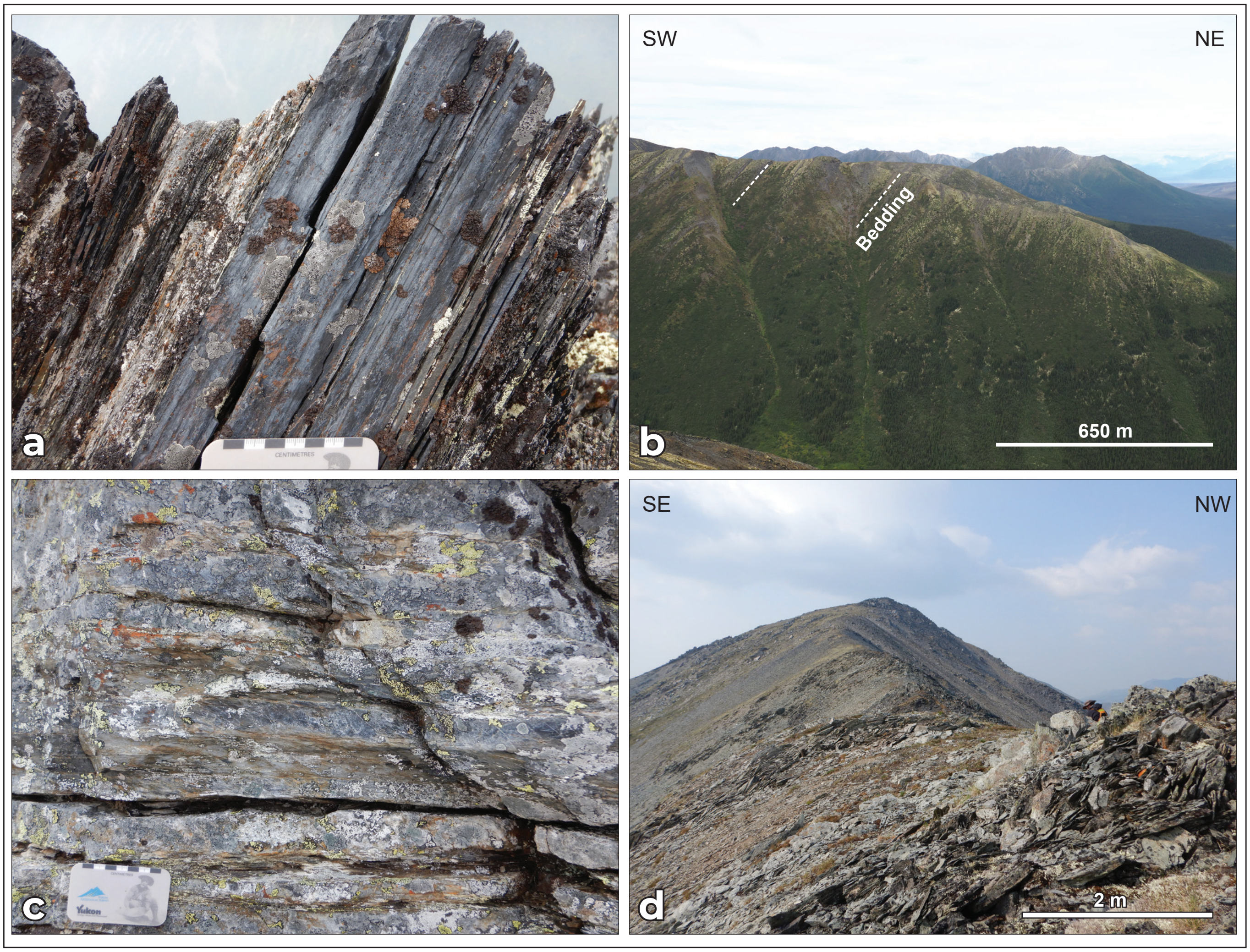

Figure 4. *Field photographs of the shale and siltstone-dominated units in the Cryogenian-Ediacaran Yusezyu Formation (Hyland Group).* ***(a)*** *Grey to dark grey, laminated mudstone (shale) in the Yusezyu Formation shale-dominated unit.* ***(b)*** *Ridge exposure of the Yusezyu Formation shale-dominated unit, exhibiting typical recessive weathering, with bedding dipping toward the southwest.* ***(c)*** *Rhythmically interbedded siltstone (light grey) and shale (brownish-grey) in the Yusezyu Formation siltstone-dominated unit.* ***(d)*** *Ridge exposure of the Yusezyu Formation siltstone-dominated unit, exhibiting characteristic grey weathering colour and rubbly outcrops of siltstone and shale.*

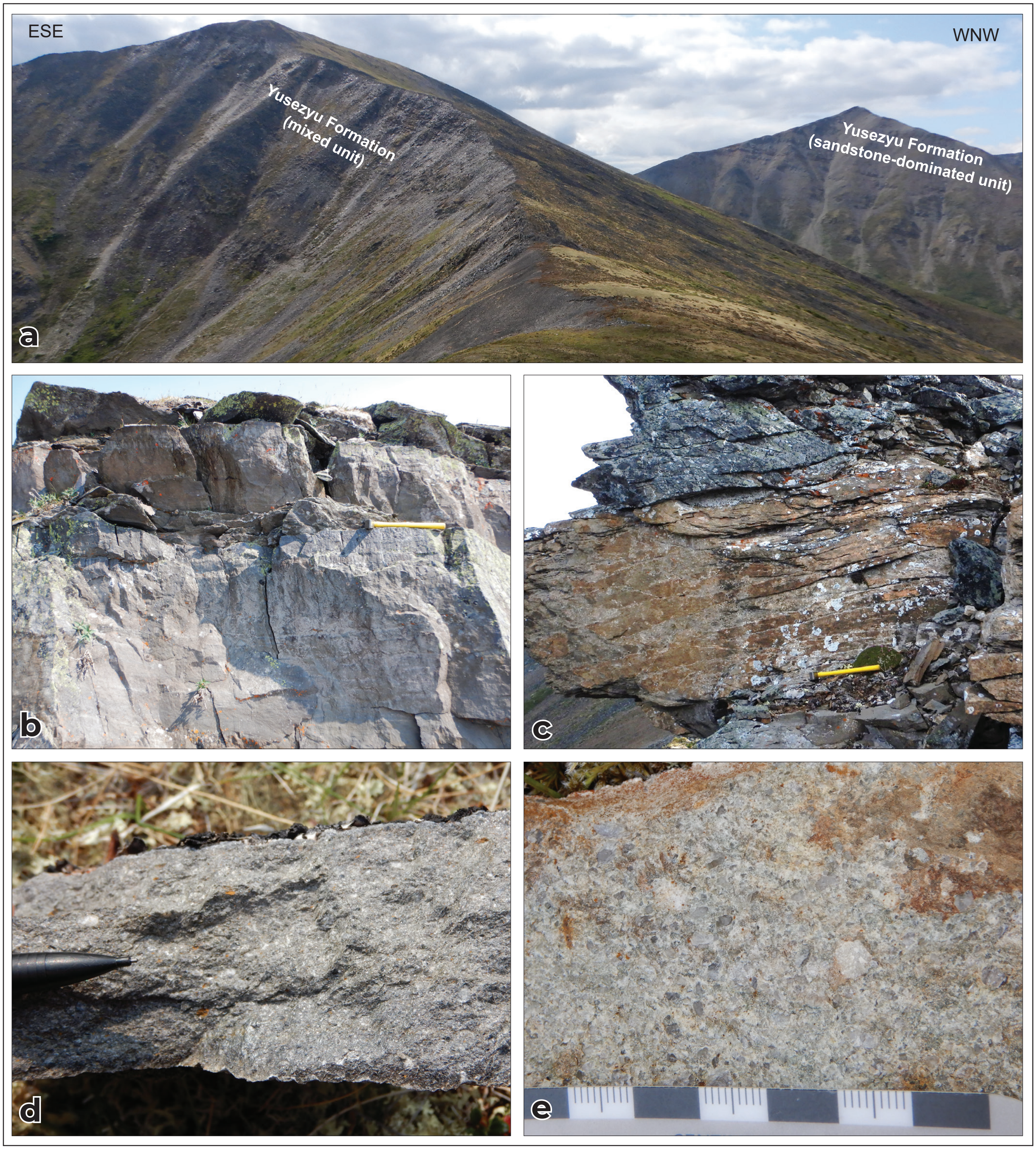

Figure 5. *Field photographs of the mixed (a) and sandstone-dominated units (a–e) in the Cryogenian-Ediacaran Yusezyu Formation (Hyland Group).* ***(a)*** *Field photograph showing recessively weathered siltstone and shale and non-recessively weathered sandstone in the Yusezyu Formation mixed unit in the foreground, and competent sandstone beds in the Yusezyu Formation sandstone-dominated unit in the background (horizontal field of view is ~3 km).* ***(b)*** *Medium to thickly bedded, brown quartz arenite.* ***(c)*** *Medium-bedded, brown-to-grey quartz arenite to quartz grit.* ***(d)*** *Brown-to-grey fresh surface of quartz arenite.* ***(e)*** *White to light grey fresh surface of quartz pebble conglomerate.*

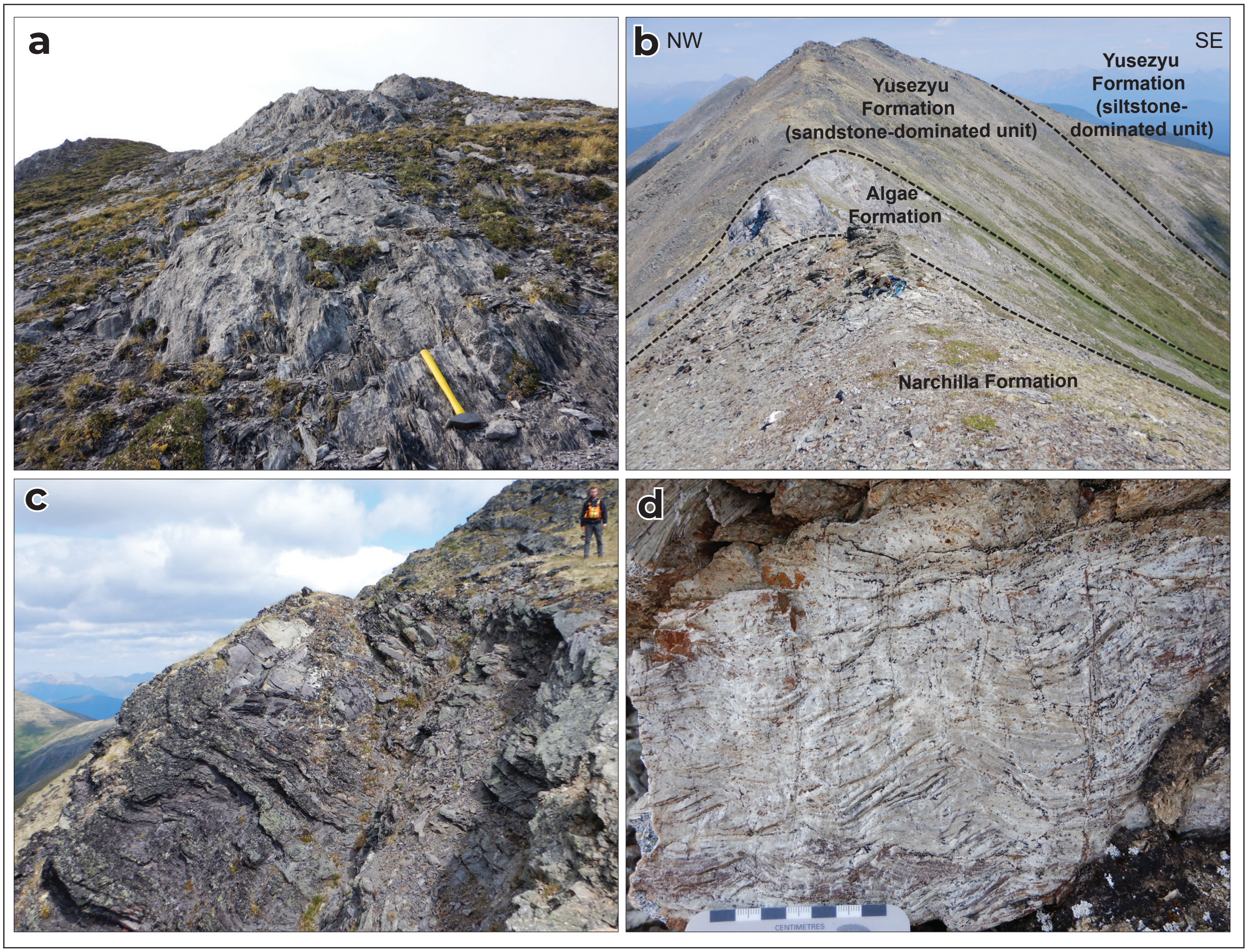

Figure 6. *Field photographs of the Ediacaran Algae Formation and the Ediacaran–Terreneuvian Narchilla Formation (Hyland Group).* ***(a)*** *Grey limestone of the Algae Formation, exhibiting a strong cleavage fabric (S2).* ***(b)*** *Light grey limestone of the Algae Formation overlain by siltstone of the Narchilla Formation and underlain by the Yusezyu Formation.* ***(c)*** *Maroon shale typical of the Narchilla Formation.* ***(d)*** *White-weathered, thinly bedded, fine-grained sandstone of the Narchilla Formation with ripple cross-laminations.*

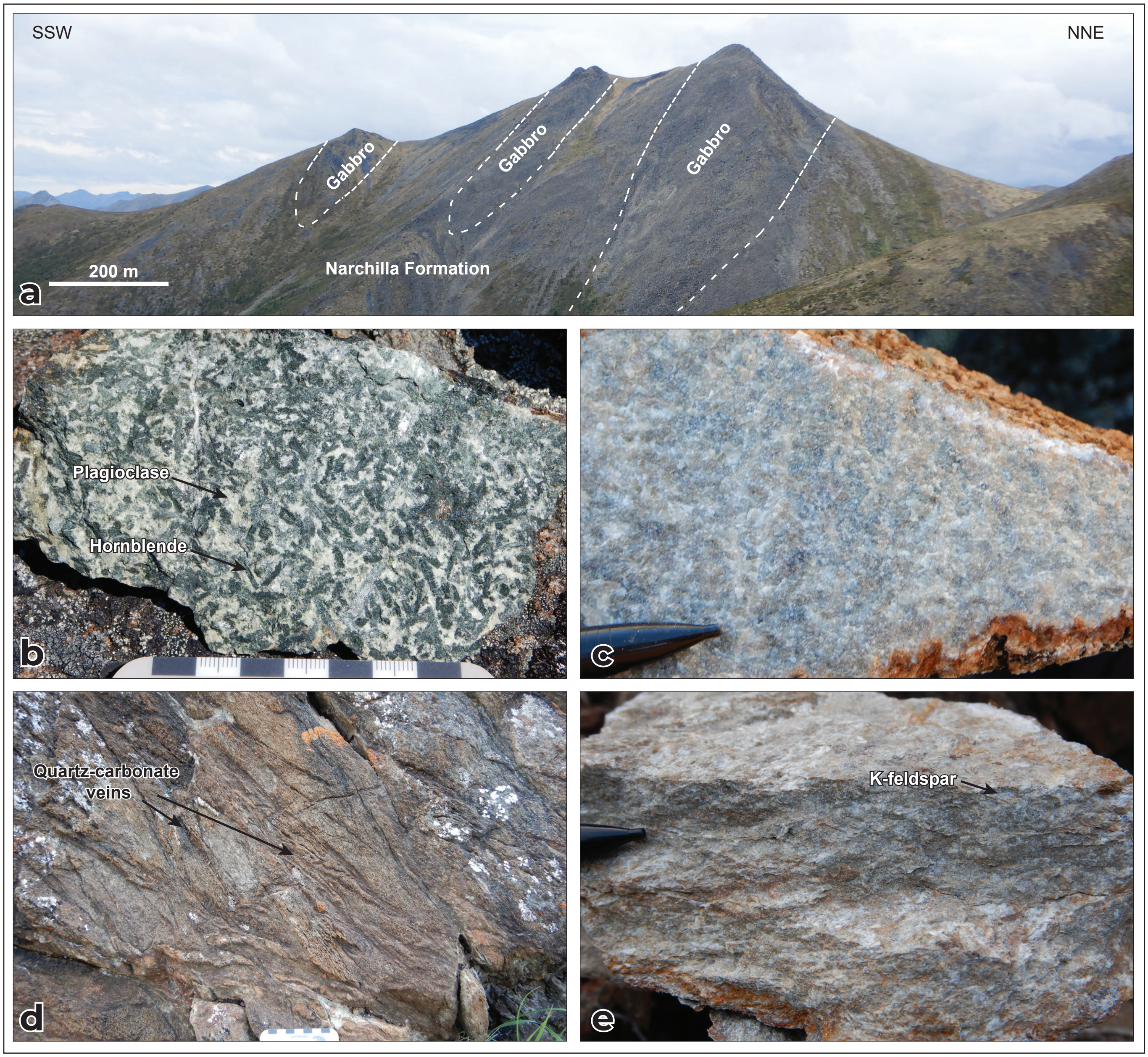

Figure 7. *Field photographs of gabbro, hornblende diorite and quartz monzonite.* ***(a)*** *Mountaintop exposure of gabbro intrusions hosted by shale and siltstone of the Narchilla Formation. Approximate gabbro contacts are represented by white dashed lines; widely spaced dashes indicate covered (inferred) contacts.* ***(b)*** *Fresh surface of medium to coarse-grained melanocratic hornblende diorite with primary igneous texture exhibited by plagioclase and hornblende. Hornblende has been mostly replaced by chlorite (sample 19DS-006-2-1 in Table 1).* ***(c)*** *Medium to coarse-grained gabbro that has been mostly replaced by greenschist-facies minerals (chlorite, epidote) and intense carbonate alteration, resulting in a pale green fresh surface that lacks igneous textures and a pitted, orange weathered surface.* ***(d)*** *Pitted, orange-brown weathered surface of quartz monzonite, with several quartz-carbonate veins.* ***(e)*** *Orange-grey fresh surface of quartz monzonite, in which original igneous minerals (e.g., K-feldspar) are barely identifiable due to intense carbonate-quartz alteration and sericitization.*

Table 1. *Whole-rock geochemical data of six gabbro and hornblende diorite samples from the Clark Lakes area. Major elements were analyzed using x-ray fluorescence (XRF) and trace elements were analyzed using inductively-coupled mass spectrometry (ICP-MS) by ALS Geochemistry.*

Sample	**19DS-006-2-1**	**19DS-007-1-1**	**19DS-034-1-1**	**19DS-040-1-1**	**19DS-111-2-1**	**19DS-115-2-1**
Lithology	**Hbl diorite**	**Gabbro**	**Gabbro**	**Gabbro**	**Gabbro**	**Gabbro**
Al_2O_3	15.29	14.90	15.08	13.61	6.69	10.67
BaO	0.02	0.02	0.01	0.01	0.01	0.03
CaO	9.83	16.00	12.15	9.60	15.55	9.85
Cr_2O_3	0.01	0.05	0.01	0.01	0.13	0.02
Fe_2O_3	15.50	8.04	12.37	17.54	8.27	16.17
K2O	0.03	0.01	0.02	0.08	0.24	0.14
MgO	5.36	8.74	5.80	4.86	5.46	8.14
MnO	0.26	0.15	0.18	0.24	1.16	0.42
Na_2O	3.15	1.93	0.44	0.52	1.08	0.05
P_2O_5	0.38	0.05	0.65	0.27	0.16	1.98
SiO_2	44.23	46.38	41.98	39.74	36.69	38.16
SrO	0.17	0.13	0.15	0.07	0.07	0.27
TiO_2	2.73	1.03	1.95	2.79	1.01	1.96
LOI	3.18	2.23	8.34	9.77	22.35	10.73
Total	101.35	99.83	99.28	99.34	99.17	99.06
Ba	69.30	61.60	27.80	25.30	44.20	240.00
Ce	64.50	23.90	102.50	44.70	17.10	1260.00
Cr	10.00	310.00	20.00	<10	930.00	90.00
Cs	0.09	0.08	0.07	0.22	0.68	0.43
Dy	5.63	2.79	6.03	4.44	1.88	39.20
Er	2.86	1.13	2.83	2.10	0.91	14.20
Eu	2.37	1.11	2.82	1.51	0.61	25.30
Ga	19.40	18.20	21.50	24.60	10.60	44.10
Gd	6.24	3.10	8.12	4.94	2.27	57.90
Ge	<5	<5	<5	<5	<5	<5
Hf	4.50	2.20	3.90	3.40	1.60	53.30
Ho	1.08	0.46	1.07	0.81	0.35	6.63
La	30.20	11.50	50.90	21.60	8.10	620.00
Lu	0.36	0.12	0.34	0.25	0.09	1.38
Nb	39.00	13.10	47.50	26.80	10.80	535.00
Nd	32.20	12.00	47.70	23.30	9.60	488.00
Pr	8.07	2.87	12.00	5.49	2.11	141.00
Rb	0.40	0.20	0.90	2.50	7.60	5.10
Sm	6.86	2.83	8.46	4.81	2.16	82.80

***Table 1** continued. Whole-rock geochemical data of six gabbro and hornblende diorite samples from the Clark Lakes area.*

Sample	**19DS-006-2-1**	**19DS-007-1-1**	**19DS-034-1-1**	**19DS-040-1-1**	**19DS-111-2-1**	**19DS-115-2-1**
Lithology	**Hbl diorite**	**Gabbro**	**Gabbro**	**Gabbro**	**Gabbro**	**Gabbro**
Sn	1.00	1.00	2.00	2.00	1.00	8.00
Sr	1605.00	1245.00	1405.00	661.00	644.00	2610.00
Ta	2.30	0.70	2.10	1.50	2.00	30.40
Tb	1.01	0.45	1.04	0.71	0.32	7.99
Th	2.51	1.42	6.12	3.14	0.91	46.60
Tm	0.36	0.16	0.34	0.25	0.10	1.81
U	0.65	0.31	1.67	1.18	0.44	18.00
V	495.00	244.00	288.00	598.00	80.00	42.00
W	<1	1.00	2.00	2.00	1.00	2.00
Y	28.10	12.60	29.10	21.40	9.30	159.00
Yb	2.27	1.09	2.57	1.67	0.71	10.20
Zr	181.00	82.00	201.00	153.00	57.00	2880.00
As	30.90	6.60	5.80	2.20	1.00	0.50
Bi	0.01	0.29	0.09	0.04	0.06	0.11
Hg	0.01	0.01	<0.005	<0.005	<0.005	0.05
In	0.01	0.01	0.02	0.05	0.03	0.23
Re	0.00	<0.001	<0.001	<0.001	<0.001	<0.001
Sb	0.32	0.50	0.07	0.05	0.05	0.29
Sc	3.00	4.00	5.70	15.60	9.80	2.10
Se	0.80	0.70	<0.2	<0.2	<0.2	0.20
Te	0.01	0.10	0.01	0.01	<0.01	0.03
Tl	<0.02	<0.02	<0.02	<0.02	<0.02	<0.02
Ag	<0.5	<0.5	<0.5	<0.5	<0.5	<0.5
Cd	<0.5	<0.5	<0.5	<0.5	0.60	<0.5
Co	61.00	32.00	40.00	62.00	77.00	16.00
Cu	169.00	233.00	136.00	143.00	30.00	9.00
Li	40.00	40.00	160.00	140.00	60.00	100.00
Mo	1.00	<1	<1	1.00	<1	<1
Ni	50.00	167.00	67.00	63.00	1110.00	78.00
Pb	9.00	96.00	36.00	28.00	62.00	20.00
Sc	19.00	53.00	18.00	22.00	11.00	2.00
Zn	142.00	43.00	105.00	184.00	159.00	401.00

Hbl = hornblende

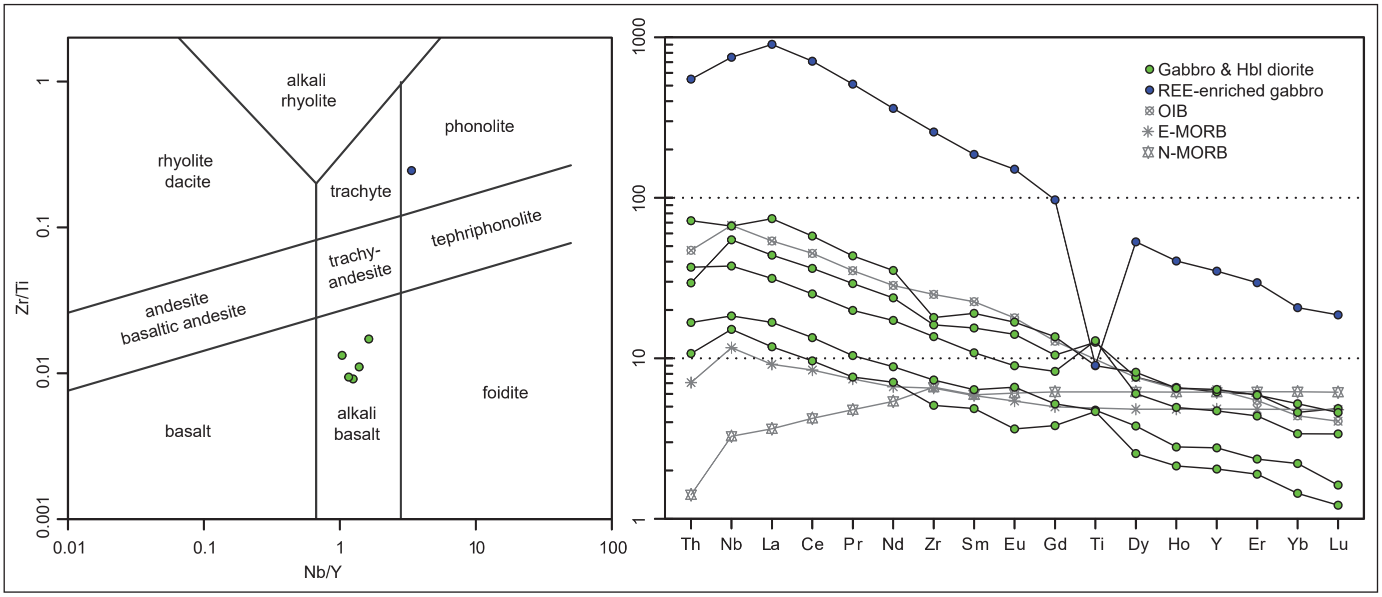

***Figure 8.** Whole-rock geochemical compositions of gabbro and hornblende diorite samples from the Clark Lakes area plotted on **(a)** the classification diagram of Pearce (1996) and **(b)** a diagram showing selected rare earth and high field strength elements normalized to the primitive mantle values of Sun and McDonough (1989). In **(b)**, compositions of oceanic island basalt (OIB), enriched mid-ocean ridge basalt (E-MORB) and normal mid-ocean ridge basalt (N-MORB) are from Sun and McDonough (1989). REE, rare earth elements; Hbl, hornblende.*

Quartz monzonite

Foliated quartz monzonite (Dqm) was observed in the southern part of the map area, hosted in siltstone of the Yusezyu Formation mixed unit (Fig. 3). The geometry and extent of the quartz monzonite are poorly defined, mainly owing to heavy vegetation in the area. It consists of medium to coarse-grained K-feldspar, plagioclase feldspar and minor quartz, and has undergone pervasive carbonate and quartz alteration. The quartz monzonite has an orange-grey fresh surface, a pitted, orange-brown weathered surface, and contains abundant carbonate (± quartz) veins (Fig. 7d,e). At the micro-scale, K-feldspar commonly exhibits microcline (“tartan”) twinning, and K-feldspar and plagioclase are strongly sericitized.

Metamorphism

The Clark Lakes area has undergone regional metamorphism at lower-greenschist-facies conditions. The siliciclastic rocks are characterized by metamorphic mineral assemblages containing white mica and chlorite (± epidote). In places in the southeastern quadrant of the map area, siltstone and phyllite also contain chloritoid porphyroblasts that are up to 1.5 mm long, or euhedral magnetite porphyroblasts up to 2 mm in diameter. Siltstone, shale and phyllite throughout the map area commonly contain ~0.5–2 mm-sized, brown to reddish-brown nodules/porphyroblasts with various shapes, including oval, rhombic, and irregular (blocky or patchy). Based on thin section analysis, at least some of these growths represent carbonate that has been partially to entirely replaced by (commonly Fe-rich) alteration assemblages, whereas others may represent altered pyrite. Pristine, euhedral carbonate rhombs occur locally. Carbonate is interpreted to have grown in the siliciclastic rocks as diagenetic nodules, or as porphyroblasts during lower-greenschist-facies metamorphism. In carbonate rocks, metamorphic minerals include white mica and, locally, tremolite, together with recrystallized calcite (and/or dolomite). In gabbro and diorite, metamorphic mineral assemblages consist of chlorite, epidote, actinolite, calcite and white mica (± titanite ± apatite). Quartz monzonite contains secondary white mica and chlorite that are consistent with lower-greenschist-facies metamorphism. The metamorphic mineral assemblages throughout the area indicate regional lower-greenschist-facies (chlorite zone) metamorphism (e.g., Spear, 1993).

Gabbro-to-diorite intrusions are surrounded by contact metamorphic aureoles in siltstone and shale host rocks. The aureoles are up to 2 m wide, and are characterized by a light green colour and a spotted hornfels texture formed by ~1–2 mm-wide, grey, oval-shaped porphyroblasts. Thin sections reveal that the original porphyroblastic mineral (possibly cordierite) has been replaced by aggregates of chlorite and quartz during regional lower-greenschist-facies metamorphism.

Deformation

On the geological compilation map of Yukon (Yukon Geological Survey, 2020a), the Dawson thrust cuts through Clark Lakes area, juxtaposing the Yusezyu Formation over the Carboniferous Tsichu(?) Formation (Fig. 2). However, 1:50 000-scale mapping at this location found no structural evidence of the Dawson fault, nor any juxtaposition of the Yusezyu and Tsichu formations. Instead, the formerly-defined trace of the Dawson fault corresponds approximately with the gradational stratigraphic boundary between the shale-dominated unit and the overlying siltstone-dominated unit in the Yusezyu Formation (Fig. 3). Grey to green shale of the Yusezyu Formation shale-dominated unit is distinct from the Tsichu Formation, which consists of black to silvery shale, carbonaceous phyllite and quartzite (e.g., Abbott, 1990a,b; Roots, 1997). Therefore, the Dawson thrust zone is projected to lie ~3 km farther to the northeast, along the valley that borders the main mountain range in the Clark Lakes area, which corresponds to a distinct linear feature on aeromagnetic maps (Figs. 3 and 9; Kiss, 2020).

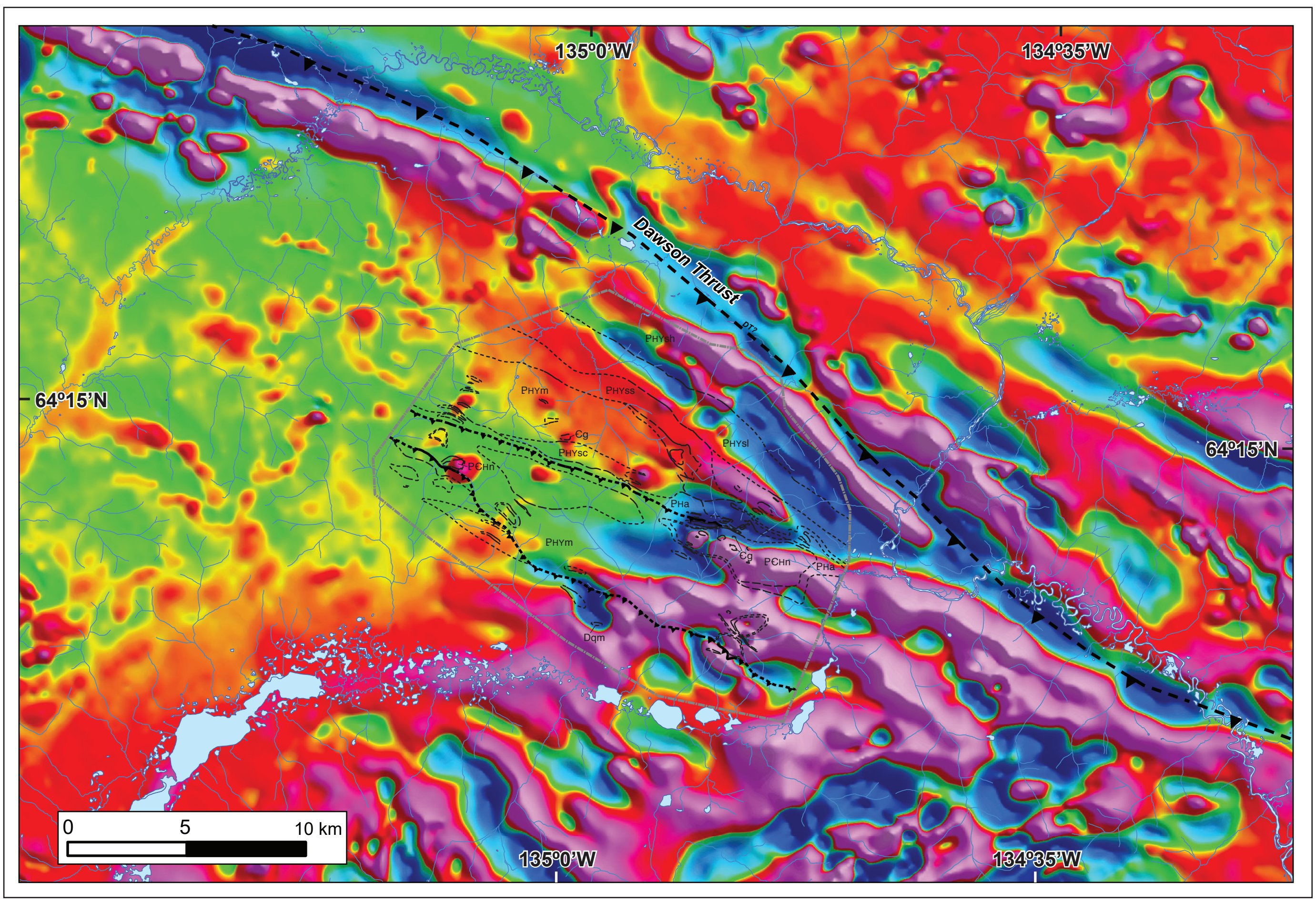

Figure 9. *Aeromagetic data (first vertical derivative; Kiss, 2020) overlain by geological contacts and faults from 1:50 000-scale mapping of the Clark Lakes area (Fig. 3a). The trace of the Dawson thrust in this figure is inferred primarily from the aeromagnetic data of Kiss (2020).*

Two regional foliations (S1 and S2) were identified during mapping of the Clark Lakes area. The sedimentary rocks exhibit a bedding-parallel foliation (S1) defined primarily by the alignment of very fine grained white mica and chlorite. Bedding and S1 are mostly southwest-dipping, although they dip with variable steepness towards both the southwest and northeast (Figs. 10a,b,e and 11a,b) as a result of later folding (F2).

The S1 foliation is crosscut by a southwest-northeast-dipping foliation (S2; Figs. 10a,b and 11c) defined by aligned fine-grained white mica (± chlorite), which commonly presents as a crenulation cleavage. The S2 foliation is generally steeply dipping, and is interpreted to have formed as an axial planar cleavage to folds (F2) with northwest-southeast-striking axial planes (Figs. 3 and 10c,e). F2 fold axes and crenulation lineations (L2) generally plunge shallowly towards the northwest or southeast (Figs. 10c,d and 11e,f). At the micro-scale, F2 folds form symmetric or asymmetric crenulations with wavelengths as small as 0.25 mm, which define a crenulation cleavage (S2). At the outcrop-scale, the F2 folds have wavelengths of ~30–60 cm (Fig. 10c), and include various types: open and close; symmetric and asymmetric; cylindrical and non-cylindrical; harmonic and disharmonic; upright to inclined; and parallel and kink folds. Larger F2 folds are common (Figs. 3 and 10e), with wavelengths ranging from <10 m to 10s of metres, and they also form map-scale folds (e.g., with wavelengths of ~0.5–3 km).

The variable dip directions exhibited by the S2 foliation, from steeply southwest to northeast, are attributed to the compounded effects of cleavage fanning and refraction in lithologic units of variable competencies (e.g., shale vs. siltstone vs. sandstone). In many places, the S2 foliation is oblique to bedding (and S1) at angles of up to 90°, a relationship that is typical of axial planar cleavage that formed in fold hinge zones (Fig. 10a,b), as well as in limbs of inclined folds. The S2 crenulation cleavage in some fine-grained rocks is sufficiently penetrative and so tightly spaced that bedding (and S1) is not discernable (or is only identifiable microscopically), precluding measurements of bedding-cleavage relationships in the field. In rocks that record only one foliation, and it is uncertain whether it is S1 or S2, the foliation is denoted "Sn" (Fig. 11d). Conversely, rocks in some places record only a bedding-parallel foliation (S1), and lack a late, non-bedding parallel foliation (S2), even at the micro-scale. This local absence of S2 is not grain-size, lithology or competency-dependent, suggesting that S2 may not be uniformly pervasive or penetrative throughout different stress-strain regimes within F2 folds. It is also possible that S2 is locally bedding-parallel, such that it transposes and is indistinguishable from S1 (e.g., in the limbs of isoclinal folds and/or in upright limbs of inclined folds).

The structural architecture of the Clark Lakes area is dominantly controlled by map-scale F2 folds, which have preserved upper stratigraphic levels, including the Algae and Narchilla formations, in synclinal keels (Figs. 3 and 10e). In several places, the underlying upper Yusezyu Formation is revealed in the cores of anticlines. Together with topographic relief, lateral facies changes and the non-cylindrical nature of the F2 folds, these relationships result in discontinuous lateral exposures of the Algae and Narchilla formations and the sandstone-dominated units in the Yusezyu Formation (Fig. 3a). Additionally, D2 thrust faults have locally transported the upper Yusezyu Formation to higher stratigraphic levels, such as above the Algae Formation (Figs. 3 and 10f). Thrust displacements are estimated to have been less than ~150 m, verging toward the northeast.

Gabbro-to-diorite intrusions exhibit a weak to moderate, southwest-to-northeast-dipping foliation that is localized along intrusion margins. Quartz monzonite exhibits a strong, southwest-dipping foliation defined mainly by the alignment of flattened K-feldspar and plagioclase grains. Microscopically, the K-feldspar and plagioclase grains exhibit undulose extinction and evidence of dynamic recrystallization and boudinage. As the gabbro-to-diorite intrusions and quartz monzonite each record only one foliation, it is uncertain whether the foliation is S1 or S2.

Both the S1 and S2 foliations are defined by lower greenschist-facies minerals and, therefore, they are both interpreted to have developed at lower-greenschist-facies conditions. Quartz in siliciclastic samples exhibits dynamic recrystallization textures, including grain boundary bulging, consistent with deformation under lower greenschist-facies conditions (e.g., Vernon, 2004).

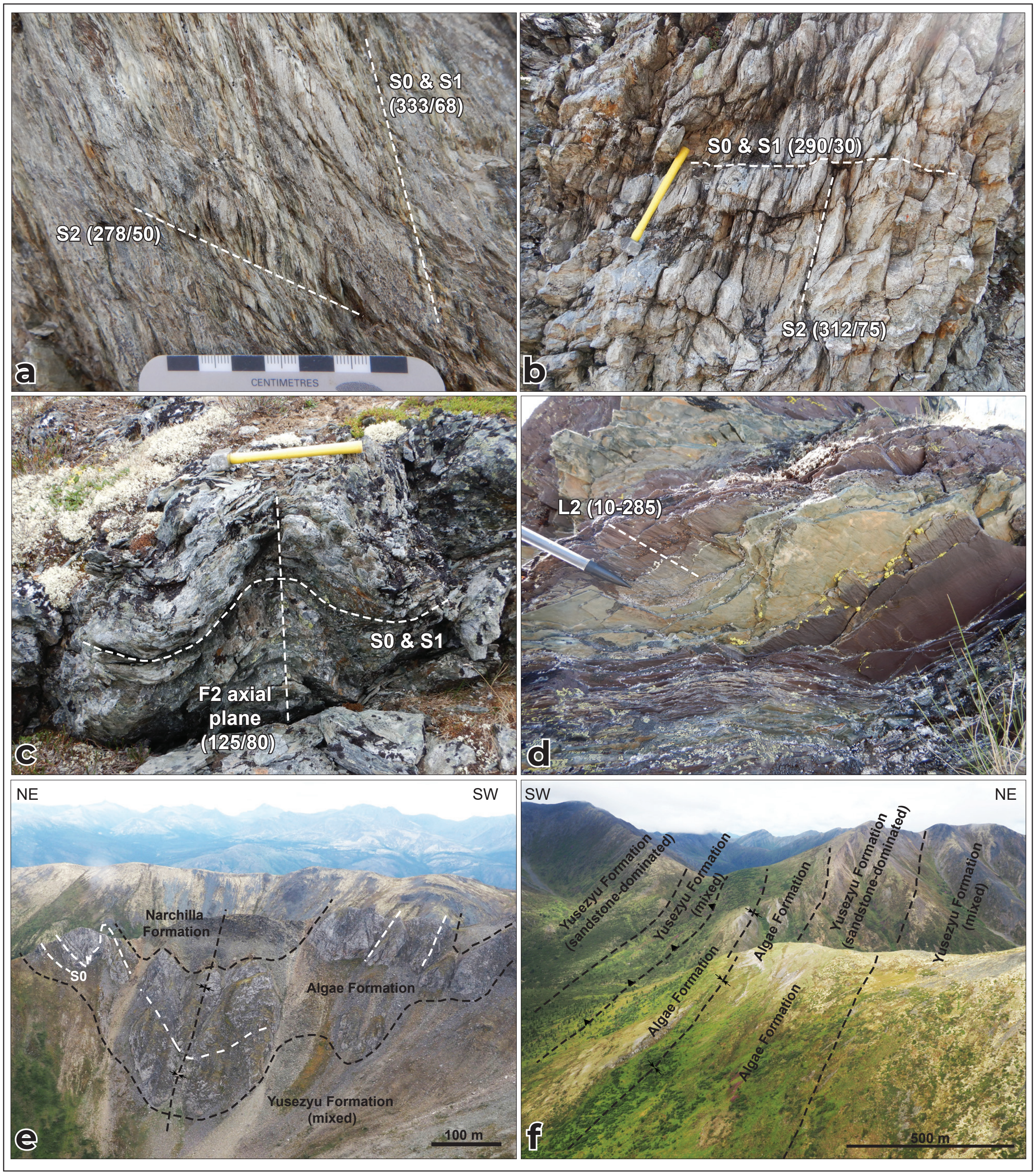

Figure 10. *Field photographs of structural relationships and deformation fabrics. Planar fabric orientations are presented in right-hand-rule format.* ***(a)*** *Bedding (S0) and bedding-parallel foliation (S1) crosscut by S2 cleavage in thinly interbedded siltstone (Narchilla Formation).* ***(b)*** *Bedding (S0) and bedding-parallel foliation (S1) crosscut by spaced cleavage (S2) in siltstone to fine-grained sandstone in the hinge zone of a map-scale synclinal F2 fold (Narchilla Formation).* ***(c)*** *An upright, open F2 fold in siltstone (Yusezyu Formation mixed unit), with a southeast-plunging axis (36–125).* ***(d)*** *Crenulation lineations (L2) in maroon to light-green shale (Yusezyu Formation mixed unit).* ***(e)*** *Cliff exposure of F2-folded rocks of the Yusezyu, Algae and Narchilla formations. The geometry of the fold is broadly synclinal, and smaller folds occur within the limbs of the syncline. The white dashed lines represent bedding traces; widely spaced dashes indicate low confidence in bedding orientations.* ***(f)*** *Panoramic view looking towards the northwest along a thrust fault that juxtaposed the Yusezyu Formation over the Algae Formation.*

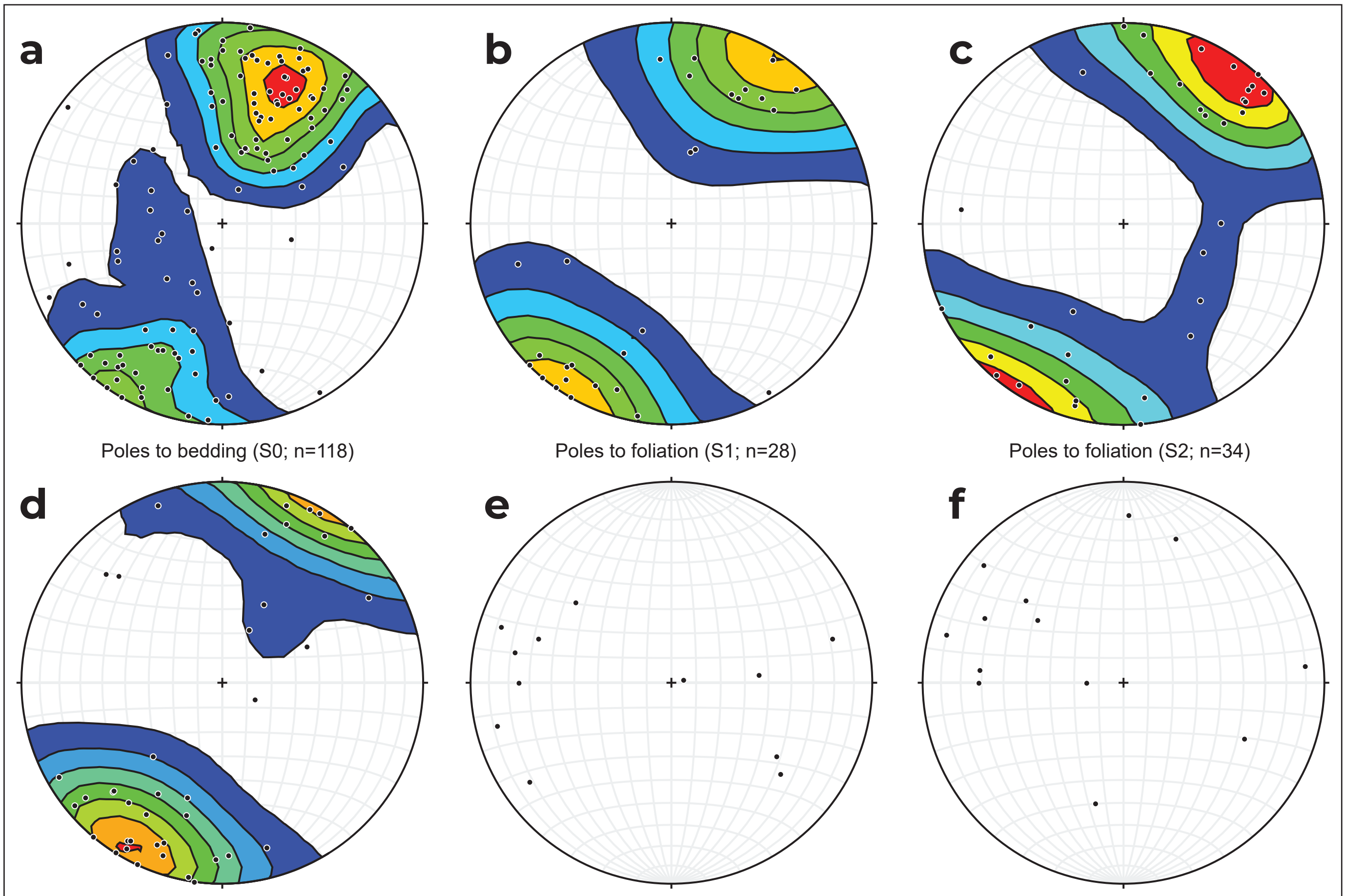

Figure 11. *Structural data from the Clark Lakes area plotted on equal-area projection stereonets (using Stereonet 10.0 software; R. Allmendinger, 2018). Data density distributions are represented by Kamb contours, for which the increasing warmth of contour colours corresponds to higher data density. (a) Poles to bedding (S0).* ***(b)*** *Poles to bedding-parallel foliation (S1).* ***(c)*** *Poles to S2 foliation, which crosscuts bedding and the bedding-parallel S1 foliation.* ***(d)*** *Poles to foliation of uncertain generation (Sn; i.e., S1 or S2; refer to text for details).* ***(e)*** *F2 fold axes.* ***(f)*** *L2 crenulation lineations. n, number of measurements.*

In summary, relationships between metamorphism and deformation suggest that the Clark Lakes area underwent burial to lower-greenschist-facies conditions, forming a bedding-parallel foliation (S1). Subsequent F2 folding and thrusting produced a crenulation cleavage (S2) at lower-greenschist-facies conditions. The orientations of D2 folds, thrusts and fabrics suggest that D2 formed during northeast-vergent shortening, which may have been related to major southeast-striking thrusts that border the Clark Lakes area. Given the northwest-vergent shear fabrics in the Tombstone high-strain zone (Murphy, 1997), it may be more likely that D2 deformation in the Clark Lakes area was related to the Dawson thrust rather than to the Tombstone and Robert Service thrusts. Notably, the thermal peak in the Clark Lakes area is higher-grade than the sub-greenschist-facies conditions recorded in stratigraphically equivalent rocks to the east beneath the Dawson thrust zone in the eastern Wernecke Mountains (Read *et al.*, 1991; Moynihan, 2014). The higher thermal peak conditions in the Clark Lakes area may have resulted from burial beneath the Tombstone and Robert Service thrust sheets.

Mineralization

As several Au and polymetallic mineral deposits occur within an ~30 km radius (Fig. 2), there is heightened interest in the Clark Lakes region; it has been classified as "prospective" to "highly prospective" by mineral potential models (Bullen, 2020). The Hyland Group has the potential to host mineral deposits, as demonstrated by the past-producing polymetallic (Ag-Pb-Zn) manto-style Clark deposit in Hyland Group limestone, located ~5 km south of the Clark Lakes map area (Fig. 2). The McKay Hill polymetallic vein Ag-Au-Pb-Zn deposit, which lies ~15 km along-strike from the Clark Lakes map area (Fig. 2), is hosted by siliciclastic and volcanic rocks that have been tentatively assigned to the Cambrian to Silurian Marmot Group (refer to Yukon MINFILE 106D 038).

Minor occurrences of sulphide mineralization were encountered during 2019 mapping of the Clark Lakes area (Fig. 12). The Narchilla Formation and the mixed and sandstone-dominated units of the upper Yusezyu Formation host quartz veins in several locations, which range in width from <1cm to ~20 cm and, less commonly, up to ~2 m (Fig. 12a). Some quartz veins are surrounded by orange, gossanous weathering and contain pyrite, or a red-brown alteration material, which may be limonite. Quartz veins are mostly discontinuous on the outcrop

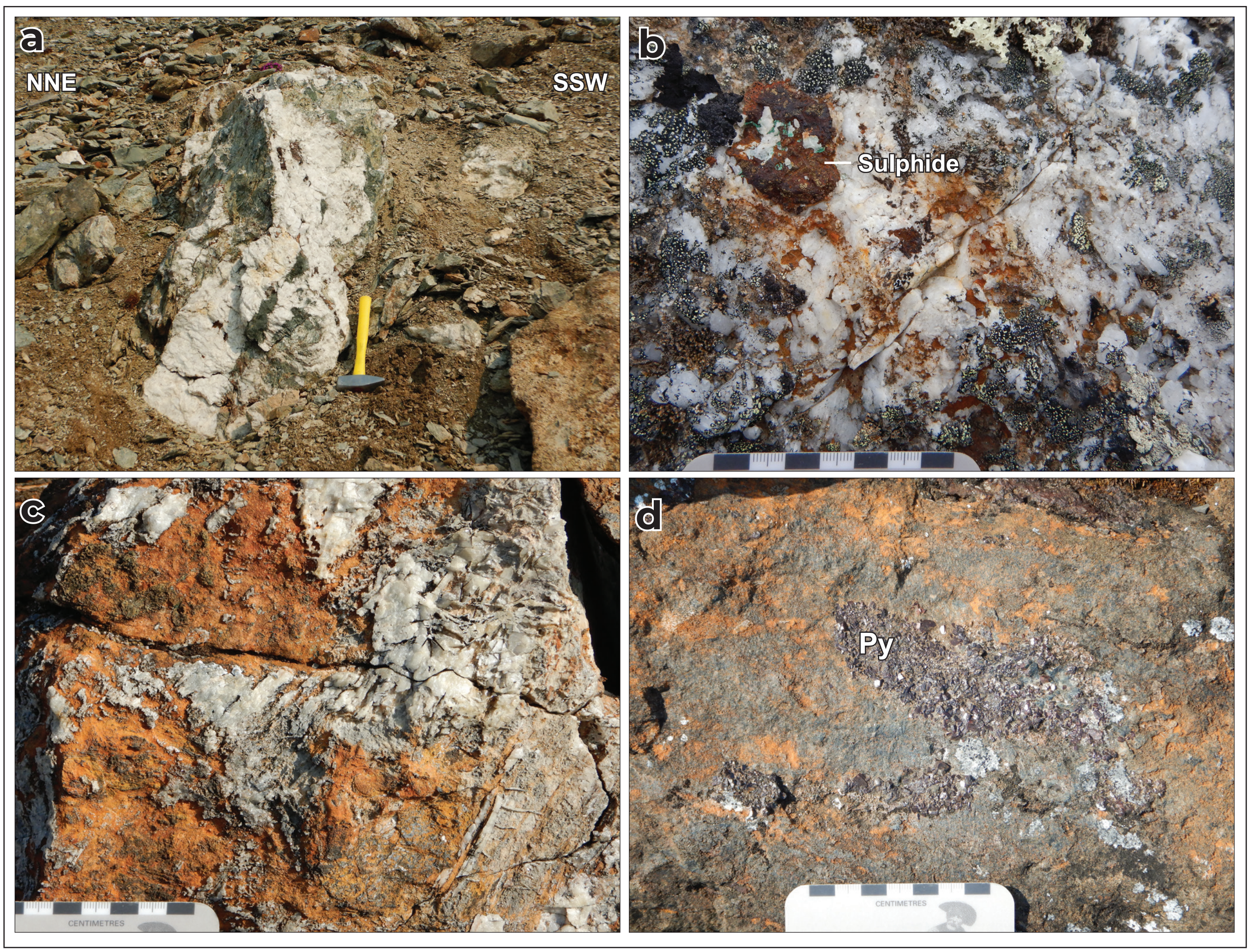

Figure 12. *Field photographs of quartz veins and sulphides hosted in the Hyland Group and gabbro in the Clark Lakes area.* ***(a)*** *A west-northwest-striking, ~1 m wide quartz vein hosted in green phyllite of the Narchilla Formation. The vein contains chlorite, carbonate, and minor rust-coloured alteration material (limonite?).* ***(b)*** *Red-brown-weathered sulphide (likely pyrite) in a 2–3 m wide quartz vein hosted in gabbro.* ***(c and d)*** *Quartz-carbonate veins hosted in orange-weathered carbonate near gabbro, with locally associated pyrite.*

scale, with some exceptions that are continuous over at least ~10 m. They have various orientations and locally form meandering networks, but they dominantly trend northwest–southeast, parallel to the regional structural grain (Fig. 12a). Siliciclastic rocks at various stratigraphic levels in the Yusezyu Formation exhibit discrete zones of silica alteration, which are up to 10s of metres wide and are generally northwest-southeast striking. This silica alteration is commonly associated with quartz veining and, in some places, with cataclastic texture. The silica-altered rocks have a distinctive white to light grey weathered surface, and a fresh surface that is either white with a "bleached" appearance or, less commonly, dark grey with the "siliceous" appearance of crystalline quartz. The predominant northwest-southeast strike of quartz veins and zones of silica alteration suggests that hydrothermal fluid flow and related mineralization were controlled—at least in part—by the northwest–southeast-striking structural grain of the area. Determining the style, architecture and timing of D2 deformation may help to understand fluid flow along the Dawson and Tombstone-Robert Service fault corridors and, therefore, the setting of hydrothermal mineral deposits in the region.

Quartz veins are also hosted by some gabbro intrusions in the Clark Lakes area. Gabbro on the eastern side of the 2019 map area hosts an ~2–3 m-wide quartz vein that contains minor pyrite (Fig. 12b). On the west side of the map area, an ~100 m wide interval of orange-weathered subcrops and rubble is interpreted to represent a skarn-like alteration zone coinciding with an intrusive contact between gabbro and the Algae Formation. Both gabbro and carbonate exhibit orange, locally gossanous weathering, and contain abundant quartz-carbonate veins with local pyrite (Fig. 12c,d).

The occurrence of quartz monzonite along the southern boundary of the area mapped in 2019 (Fig. 3a) raises the possibility of intrusion-related mineralization in the area. The quartz monzonite may share affinity with other felsic igneous rocks in the region (Fig. 2), some of which are associated with mineral deposits, including the Rackla granite (*ca.* 63–59 Ma; Kingston et *al.*, 2010) at the Tiger Au deposit, or the Dublin Gulch pluton (*ca.* 93.5–92.8 Ma; Murphy, 1997) at the Eagle Au Mine, which belongs to the Mayo Suite plutons (*ca.* 94–93 Ma; Hart et *al.*, 2004). Alternatively, if the quartz monzonite was deformed during the mid-Cretaceous (*e.g.*, by *ca.* 104–100 Ma deformation associated with the Tombstone high-strain zone; Mair et *al.*, 2006), it may share affinity with older felsic rocks, such as ca. 380–378 Ma (Murphy, 1997) felsic volcanic rocks in the Earn Group, host to the Marg volcanogenic massive sulphide deposit (Fig. 2).

Magnetic susceptibility

To facilitate geophysical interpretations, magnetic susceptibility measurements were obtained for major lithologic units at 150 sites across the Clark Lakes area in 2019. In total, 162 measurements were acquired using a ZH Instruments SM-30 Magnetic Susceptibility Meter. Each "measurement" is the average of five individual measurements from each lithology. Magnetic susceptibilities of the sedimentary rocks ranged from 0.01 to 0.2 SI units, whereas those of gabbro-to-diorite intrusions were typically between 0.2 and 0.5 SI units. Magnetite-bearing siltstone in the southeastern part of the map area produced elevated values of 1.00 to 50.0 SI units.

Acknowledgements

Maurice Colpron, Rosie Cobbett and David Moynihan and the Yukon Geological Survey bedrock geology group are thanked for field visits and helpful discussions. Julia Lane and Adam Coulter of ATAC Resources Ltd. are gratefully acknowledged for their logistical support. Transportation during fieldwork was provided by Horizon Helicopters. David Moynihan and Maurice Colpron are thanked for their helpful reviews of this article. Fieldwork was conducted in the traditional territory of the First Nation of Na-Cho Nyäk Dun.

References

Abbott, G., 1990a. Geological map of Mt. Westman map area (106D/1). Exploration and Geological Services Division, Yukon Region, Indian and Northern Affairs Canada, Open File 1990-1, scale 1:50 000.

Abbott, G., 1990b. Preliminary results of the stratigraphy and structure of the Mt. Westman area, central Yukon. Geological Survey of Canada, Current Research 1990-1E, p. 15–22.

Abbott, G., 1997a. Geology of NTS map area 116A/10, eastern Ogilvie Mountains, Yukon. Exploration and Geological Services Division, Yukon Region, Indian and Northern Affairs Canada, Geoscience Map 1997-2, scale 1:50 000.

Abbott, G., 1997b. Geology of Two Beaver Lake map area, eastern Ogilvie Mountains, Yukon (NTS 116A/11). Exploration and Geological Services Division, Yukon Region, Indian and Northern Affairs Canada, Geoscience Map 1997-3, scale 1:50 000.

Abbott, G., 1997c. Geology of the Upper Hart River Area, Eastern Ogilvie Mountains, Yukon Territory (116A/10, 116A/11). Exploration and Geological Services Division, Yukon Region, Indian and Northern Affairs Canada, Bulletin 9, 92 p.

Allmendinger, R., 2018. Stereonet 10.0. Cornell University, http://www.geo.cornell.edu/geology/faculty/RWA/programs/stereonet.html, [accessed November 20, 2020].

Anderson, R.G., 1987. Plutonic rocks in the Dawson map area, Yukon Territory. Geological Survey of Canada, Current Research 1987-1A, p. 689–697.

Bullen, W., 2020. New mineral potential mapping methodology for Yukon: Case studies from the Beaver River and Dawson regional land use planning areas. *In*: Yukon Exploration and Geology 2019, K.E. MacFarlane (ed.), Yukon Geological Survey, p. 23–42.

Colpron, M., Moynihan, D., Israel, S. and Abbott, G., 2013. Geological map of the Rackla belt, east-central Yukon (NTS 106C/1–4, 106D/1). Yukon Geological Survey, Open File 2013-13, 1:50 000 scale, 5 maps and legend.

Colpron, M., Nelson, J.L. and Murphy, D.C., 2007. Northern Cordilleran terranes and their interactions through time. GSA Today, vol. 17, no. 4/5, p. 4–10.

Green, L.H. and Roddick, J.A., 1962. Dawson, Larsen Creek, and Nash Creek map-areas, Yukon Territory (116B, C, E1/2, 116A and 106D). Geological Survey of Canada, Paper 62-7, 20 p., plus maps.

Green, L.H., 1972a. Geology, Nash Creek, Yukon Territory. Geological Survey of Canada, Department of Energy, Mines and Resources, Map 1282A, scale 1:250 000.

Green, L.H., 1972b. Geology of Nash Creek, Larsen Creek, and Dawson map-areas, Yukon Territory (106D, 116A, 116B, and 116C (E1/2)). Geological Survey of Canada, Memoir 364, 157 p.

Hart, C.J.R., Goldfarb, R.J., Lewis, L.L. and Mair, J.L., 2004. The Northern Cordilleran mid-Cretaceous plutonic province: Ilmenite/magnetite-series granitoids and intrusion-related mineralisation. Resource Geology, vol. 54, p. 253–280.

Kingston, S., Mortensen, J.K., Dumala, M. and Gabites, J., 2010. Ar-Ar geochronology and Pb isotopic constraints on the origin of the Rau gold-rich carbonate replacement deposit, central Yukon. *In:* Yukon Exploration and Geology 2009, K.E. MacFarlane, L.H. Weston, and L.R. Blackburn (eds.), Yukon Geological Survey, p. 213–222.

Kiss, F., 2020. Aeromagnetic Survey of the Nash Creek Area, Yukon, Parts of NTS 105-M, N, 106-C, D, 115-P and 116-A. Geological Survey of Canada, Open File 8728; Yukon Geological Survey, Open File 2020-7, scale 1:100 000, https://doi.org/10.4095/326147.

Mair, J.L., Hart, C.J.R. and Stephens, J.R., 2006. Deformation history of the northwestern Selwyn Basin, Yukon, Canada: Implications for orogen evolution and mid-Cretaceous magmatism. GSA Bulletin, vol. 118, p. 304–323.

Moynihan, D., 2014. Bedrock Geology of NTS 106B/04, Eastern Rackla Belt. *In:* Yukon Exploration and Geology 2013, K.E. MacFarlane, M.G. Nordling and P.J. Sack (eds.), Yukon Geological Survey, p.147–167.

Moynihan, D., 2016a. Bedrock geology compilation of the eastern Rackla belt, NTS 105N/15, 105N/16, 105O/13, 106B/4, 106C/1, 106C/2, east-central Yukon. Yukon Geological Survey, Open File 2016-2, scale 1:75 000, 2 sheets.

Moynihan, D., 2016b. Stratigraphy and structural geology of the upper Hyland River area (parts of 105H/8, 105H/9), southeast Yukon. *In:* Yukon Exploration and Geology 2015, K.E., MacFarlane and M.G. Nordling (eds.), Yukon Geological Survey, p. 187–206.

Murphy, D.C., 1997. Geology of the McQuesten River Region, Northern McQuesten and Mayo Map Area, Yukon Territory (115P/14, 15, 16; 105M/13, 14). Exploration and Geological Services Division, Yukon Region, Indian and Northern Affairs Canada, Bulletin 6, 122 p.

Pearce, J.A., 1996. A user's guide to basalt discrimination diagrams. *In:* Trace Element Geochemistry of Volcanic Rocks: Applications for Massive Sulphide Exploration, D.A. Wyman (ed.), Geological Association of Canada, Short Course Notes, vol. 12, p. 79–113.

Read, P.B., Woodsworth, G.J., Greenwood, H.J., Ghent, E.D. and Evenchick, C.A., 1991. Metamorphic Map of the Canadian Cordillera. Geological Survey of Canada, Map 1714A, scale 1:2 000 000.

Roots, C.F., 1988. Cambro-Ordovician volcanic rocks in eastern Dawson map area, Ogilvie Mountains, Yukon. *In:* Yukon Geology, volume 2, G. Abbott (ed.), Exploration and Geological Services Division, Yukon, Indian and Northern Affairs Canada, p. 81–87.

Roots, C.F., 1997. Geology of the Mayo Map Area, Yukon Territory (105M). Exploration and Geological Services Division, Yukon Region, Indian and Northern Affairs Canada, Bulletin 7, 82 p.

Spear, F.S., 1993. Metamorphic Phase Equilibria and Pressure-Temperature-Time Paths. Mineralogical Society of America, Monograph 1, 799 p.

Sun, S.S. and McDonough, W.F., 1989. Chemical and isotopic systematics of oceanic basalts; implications for mantle composition and processes. Geological Society Special Publications, vol. 42, p. 313–345.

Tempelman-Kluit, D.J., 1970. Stratigraphy and structure of the Keno Hill quartzite in Tombstone River-Upper Klondike River map areas, Yukon Territory (116B/7, B/8). Geological Survey of Canada, Bulletin 180, 102 p. and maps.

Thompson, R.I., Roots, C.F. and Mustard, P.S., 1990. Repeated Proterozoic passive margin extension influences Late Cretaceous folding and thrusting in southern Ogilvie Mountains, Yukon. Geological Association of Canada, Program with Abstracts, vol. 15, p. 131.

Vernon, R.H., 2004. A Practical Guide to Rock Microstructure. Cambridge University Press, New York, USA, 594 p.

Yukon Geological Survey, 2020a. Yukon Digital Bedrock Geology. Yukon Geological Survey, http://data.geology.gov.yk.ca/Compilation/3#InfoTab, [accessed November 6, 2020].

Yukon Geological Survey, 2020b. Yukon Lithogeochemistry data set: Yukon Geological Survey, http://data.geology.gov.yk.ca/Compilation/35#InfoTab, [accessed October 20, 2020].